Journal of the Korean Nuclear Society
Volume 25, Number 4, December 1993

《Review》

Internal Hydriding of Defected Zircaloy Cladding Fuel Rods : A Review

Yongsoo Kim and Donald R. Olander
University of California, Berkeley, CA

Wonmok Jae
Hanyang University

(Received June 7, 1993)

결함 핵연료 피복관 내부에서의 수소 침투에 관한 개론적 고찰

김용수 · 도날드 올랜더
캘리포니아 버클리대학교
제원목
한양대학교

(1993. 6. 7 접수)

Abstract

Recently a number of severe fuel degradation events, seemingly due to internal secondary hydriding, have been reported. This paper reviews internal hydriding of defected zircaloy cladding. First, the history of zircaloy cladding development and the environment of the zircaloys in service in the nuclear reactor are introduced. Fundamental aspects of zircaloy hydriding, such as hydrogen permeability in zirconium oxide, terminal solubility and precipitation in zirconium and its alloys, and the deleterious effect of hydrides are reviewed. The mechanism of massive internal hydriding in defected zircaloy fuel rods is qualitatively described based on the observed phenomena. Significant factors affecting the hydriding process are discussed. A quantitative model for the massive hydriding as a part of an effort to mitigate fuel degradation is briefly mentioned and necessary information and recommended future work for improvement of the model are outlined.

요 약

최근 전 세계적으로 내부2차수소 침투에 의한 것으로 보이는 핵연료의 심각한 파손이 잇달아 보고되었다. 본 논문에서는 결함 핵연료에서의 내부 수소 침투 현상이 개괄적으로 고찰된다. 먼저 핵연료의 피복관으로 사용되는 질코늄 합금의 개발사와 그 질코늄 합금이 사용되는 원자로 내의 운전조건이 소개되고 산화 질코늄 막에서의 수소의 투과성, 질코늄과 질코늄 합금에서의 수소의 최종 용해도와 침전도등 질코늄의 수소 침투에 관련된 기본 사항과 수소 침투가 기계적 강도에 미치는 악 영향등이 고찰된다. 결함 핵연료봉 내부에서 발생되는 수소의 대량 내부 침투의 메카니즘이 관찰된 제 현상을 중심으로 정성적으로 설명되고 이러한 수소의 대량 침투에 의한 핵연료의 파손 심화를 줄이기 위한 노력의 일환으로 제시된 정량적 모델이 간단히 언급되고 이러한 정량적인 모델의 심도있는 개발을 위해 필요한 자료와 추후의 연구 내용이 설명된다.

1. Introduction

Hydriding of zircaloy cladding has been and continues to be one of the important causes of fuel failures in light water reactors. Operating experience of nuclear power plants shows that past capacity factor losses due to fuel failures have been principally caused by hydriding of zircaloy cladding (PWR, BWR, and PHWR) and by pellet cladding interaction (BWR)[1]. Internal hydriding of the zircaloy cladding was a persistent cause of defects and occasional fuel failures in early LWRs[2,3]. Recently fuel failures due to this internal hydriding, which released a large amounts of radioactivity, have been reported[4-6]. The occurrence of two separate fuel failures[4,5] initiated a worldwide fuel-failure survey involving over thirty utilities using BWR fuel and international cooperation on this issue. Fuel failures at Oconee unit 2 (PWR) proved to be secondary failures caused by cladding hydriding after the initial defect was formed[6]. In coming years this problem may be particularly important because of the demand of reliable high burnup fuel performance.

In this paper, the fundamental aspects of zircaloy hydriding and the mechanism of internal hydriding failures in defected zircaloy-clad fuel rods are reviewed and recommendations for future work are presented. An overview of the past operating experience on hydriding failures of zircaloy cladding as well as in-pile and out-of-pile test data will be dealt with in the next paper, in which the main causes of past fuel element failures in water-cooled power reactors are reviewed.

Parts of this paper are drawn from the reviews of Vaknin and Olander[7] and Clayton[8] on internal secondary hydriding of defected zircaloy clad fuel rods.

Development of a Zircaloy Cladding

Early U. S. power reactors used austenitic stainless steel as the fuel cladding. Chloride stress corrosion cracking of stainless steel forced the light water reactor (LWR) designers to shift to Zircaloy-2, an alloy of zirconium with tin, iron, chromium, and nickel, which became standard[9]. It was also adopted by the engineers in Canada who were designing reactors which used natural uranium, rather than enriched uranium, for fuel[10]. PWRs used a new version of zircaloy called Zircaloy-4, modified in composition to reduce absorption of hydrogen[11].

Fuel cladding for water-cooled power reactors must meet a variety of technical and economic

Table 1. Typical Reactor Environments Where Zirconium Alloys Are Used

	PWR	BWR	PHWR
outlet temperature	310~330℃	~290℃	~300℃
coolant material	H_2O	H_2O	D_2O
pressure(MPa)	~15	~7	~10
$[O_2]$(ppb)	~5	~200	<5
$[H_2]$(ppm)	2~5	~0.02	0.5~1
pH	6.9~7.4	7	10.2~10.8
neutron flux (n/cm^{2}s, E>1MeV)	10^{14}	8×10^{13}	3×10^{13}
average LHGR*	17.5kW/m	19kW/m	26kW/m
maximum LHGR*	42kW/m	44kW/m	44kW/m
	Zircaloy-4	Zircaloy-2	Zircaloy-4 [+]
			Zr-2.5Nb [++]

*Linear Heat Generation Rate [+]fuel cladding [++]pressure tube

Table 2. Composition of Various Zirconium Alloys(wt %)

Elements	Zircaloy-2	Zircaloy-4	Zr-2.5Nb	Zr-Sn-Nb-Fe*
Zr	97.5–98.5	97.9–98.5	97.5	97.9
Sn	1.2–1.7	1.2–1.7	–	1.0
Fe	0.07–0.20	0.18–0.24	–	0.1
Cr	0.05–0.15	0.07–0.13	–	–
Ni	0.03–0.08	–	–	–
Nb	–	–	2.5	1.0

*ZIRLO™ from Westinghouse Electric Corporation

challenges. It must have corrosion resistance and satisfactory strength in the operating environment of the reactor core. Typical reactor environments where zirconium alloys are in service are summarized in Table 1. Zircaloy met these general criteria and early fuel designs were based on the properties found in tubing produced around 1960. The demand for more efficient and reliable fuel has been met with optimization of basic zircaloy tubing rather than a dramatic shift to another alloy system. Only the development of the Zr-2.5% Nb alloy for Canadian pressure tubes led to a new alloy[12]; but even there, the fuel cladding remains zircaloy. In Table 2, the composition of various zirconium alloys are listed, including the Zr-Sn-Nb-Fe alloy, which is claimed to be an advanced zircaloy cladding for high burnup[13].

Three very significant discoveries made substantial impacts on the application of zircaloy in water-cooled reactors. The first was the discovery that nickel in Zircaloy-2 promoted absorption of hydrogen. This was very important in PWRs which use an overpressure of hydrogen in the reactor coolant, which adds to hydrogen generated by the corrosion reaction (Table 1). Thus a new zirconium alloy composition evolved with the nickel content of Zircaloy-2 being replaced with additional iron to maintain the desired corrosion resistance (Table 2). Continued research has resulted in the development of Zircaloy-4 which has lower hydrogen pick-up in water corrosion than does Zircaloy-2[11]. Figures 1 and 2 show hydrogen pick-ups in Zircaloy-2 and Zircaloy-4 during corrosion and the relationship of hydrogen pick-up and corrosion weight gain for Zircaloy-2 and Zircaloy-4.

The next discovery was the effect of an intermediate 'beta quench' in the manufacturing process which improved uniformity of the microstructure and reliability of corrosion performance[14,15]. Last was the effect of metal crystal orientation on the direction in which hydrides precipitated in the tubing[16,17]. Tubing made by the drawing process commonly used for steel and other tubes produced radially oriented hydrides which made the tubing brittle. Tubing made by the cold pilger or rocking process gave rise to hydride platelets that formed circumferentially around the tube

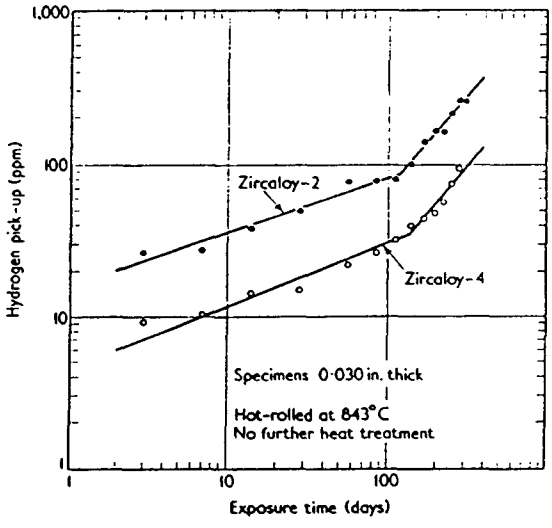

Fig. 1. Hydrogen Pick-up in Zircaloy-4 During Corrosion Reaction in 360℃ Water[11]

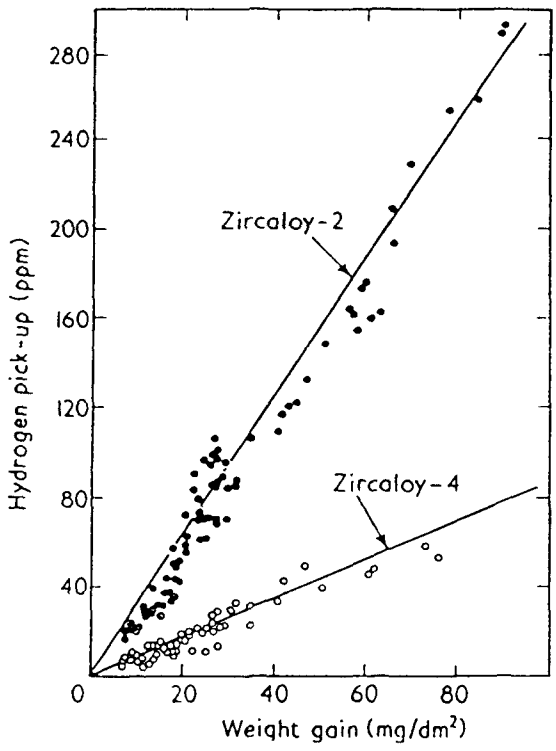

Fig. 2. Relationship of Hydrogen Pick-up and Corrosion Weight Gain for Zircaloy-2 and Zircaloy-4[11]

leaving the tube relatively ductile[18-20]. Since hydrogen was introduced into the tubing as a result of normal corrosion during service, this was a crucial effect.

There is no single set of 'best' properties for a fuel cladding tube. The properties must complement the requirements of the fuel design concept. Therefore compositions as well as manufacturing processes must be adjusted to optimize the desired properties with minimum degradation in other properties.

2. Hydriding of Zircaloy

Classification of Zircaloy Hydriding

Zircaloy hydriding is classified into two main categories according to the sources of hydrogen : external and internal.

External hydriding arises from sources of hydrogen outside the fuel element : waterside corrosion, dissolved hydrogen in coolant water and water radiolysis.

• Waterside corrosion.

The corrosion reaction of zircaloy with coolant water generates hydrogen according to :

$$Zr+2H_2O \rightarrow ZrO_2+2H_2 \quad (1)$$

Part of the hydrogen formed by this aqueous corrosion of zircaloy is absorbed by the zircaloy, which is called 'hydrogen pick-up'. The accumulated amount of hydrogen pick-up depends on the exposure time, the wall thickness of the zircaloy tubing, and the kind of zircaloy.

• Dissolved hydrogen in coolant water.

Coolant water, especially in PWRs, ordinarily contains about 25 cc H_2/kg H_2O, some of which can dissolve in zircaloy.

• Radiolysis of water.

When liquid water is irradiated with high energy radiation, decomposition occurs in two principal reactions[21] :

$$H_2O \rightarrow H+OH \quad (2a)$$

$$2H_2O \rightarrow H_2+H_2O_2 \quad (2b)$$

The relative amount of each reaction depends on the type of irradiation and the stopping power of the radiation in water. About 80% of H_2O is decomposed by gamma rays by reaction (2a) and 90% of decomposition by alpha particles or fission fragments proceeds by reaction (2b).

Internal hydriding is caused by hydrogen sources inside the fuel element. Internal hydriding is further classified as primary and secondary hydriding. Primary hydriding refers to clad hydriding in undefected elements due to internal hydrogen sources. Secondary hydriding refers to hydriding on the cladding inner surface by coolant entering inside fuel rod through an existing defect.

There are four possible sources of hydrogen for primary hydriding :

• Impurities in the helium fill gas.

• Radiolytic decomposition of organic contamination.

• Hydrogen content in fuel pellets (trapped in the pores and dissolved in UO_2 lattice)

• Moisture absorbed by the UO_2 fuel pellet (this was at one time the most significant internal source of hydrogen).

For secondary hydriding, fuel oxidation either by steam or by hydrogen peroxide from the radiolysis produces additional hydrogen :

• All the above-mentioned sources for the external hydriding.

• Steam oxidation of fuel either by steam :

$$2H_2O+2/yUO_{2+x} \rightarrow 2/yUO_{2+x+y}+2H_2 \quad (3a)$$

or by hydrogen peroxide from the radiolysis process mentioned earlier :

$$H_2O_2+2/yUO_{2+x} \rightarrow 2/yUO_{2+x+y}+H_2 \quad (3b)$$

The hydrogen produced inside zircaloy cladding is mostly absorbed by the cladding, which can evolve into a large secondary defect at the position where accelerated hydrogen pick-up occurs. Figure 3 schematically depicts the hydrogen-generating reactions in internal hydriding.

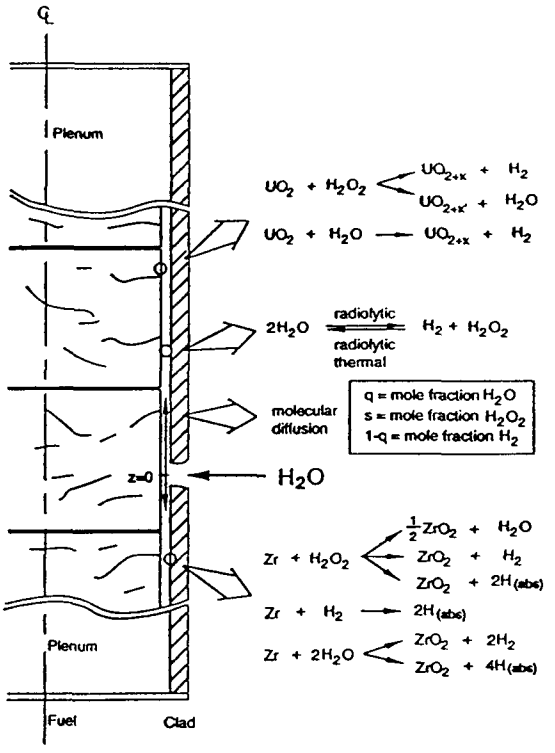

Fig. 3. Hydrogen Production Reaction in a Defected Fuel Rod

Hydrogen Pick-up and Permeation

Since Goldman and Thomas[22] demonstrated early in 1953 that a fraction of the total quantity of hydrogen generated by the zircaloy corrosion with water is absorbed by the corroding alloy along with oxide film formation, extensive research on hydrogen pick-up by zirconium and zirconium alloys has been carried out[23-32]. Also a number of studies have focused on hydrogen-pick-up-related subjects such as embrittlement of zirconium alloys, effect of environment, influence of oxide layer formation and so on.

Apart from waterside corrosion, many processes can generate hydrogen, as seen in the previous section. Once hydrogen is picked up by zirconium or a zirconium alloy it permeates the oxide layer, reaches interface between oxide and metal, and precipitates or forms hydride in the metal matrix. It is well-known that the surface oxide film is a good barrier against direct reaction of zirconium with hydrogen as long as sufficient oxidant is present to maintain an oxidizing environment[33-43]. It has been found that there exists a critical ratio of hydrogen/oxidant below which the oxide film remains protective[33,37,39,41]. This critical ratio varies with temperature, pressure, and oxidant. If the hydrogen/oxidant ratio is above the critical ratio there will be insufficient oxidant to maintain the oxide film and the rate of oxygen dissolution in the metal will exceed the rate of formation of new oxide[44,45]. The 'breakdown process' of the surface oxide film, in which dissolution of the oxide at grain boundaries occurs, leads to the formation of pores at these locations and permits direct reac-

tion of hydrogen with the metal[8]. The incubation time for the breakdown of the oxide film depends on the nature of the oxide layer (Figure 4)[35]. Hydrogen then enters the metal as a part of the corrosion reaction. The proton is discharged by electron migration through the oxide filmand the resulting H atoms either recombine to form H_2 gas or diffuse into the metal. The ratio of the rates of these two process determines the percentage hydrogen pick-up[46].

In environments of steam and hydrogen the critical $P(H_2)/P(H_2O)$ ratio was measured[3,24,28,36,37,41,42] as a function of hydrogen pressure, temperature and surface conditions. It was found for non pre-oxidized surfaces tzo be in the range of 10^2–10^6 for 350~400℃ and H_2 pressure from 0.06 up to 1 atm. Zima[24] developed the following condition that must be met for hydriding to occur in pre-filmed Zircaloy-2 in the temperature range of 300~400℃ :

$$P(H_2)/P(H_2O) \geq 6 \ |P(H_2)^{2/3} \quad (4)$$

where $P(H_2)$ is in Torr. Wide scatter of the experimental $P(H_2)/P(H_2O)$ ratios around those predicted by Equation (4) were ascribed to the influence of other variables than just the composition of the gas.

On the other hand, Studsvik AB suggested the following conditions[7] :

$$Log\ |P(H_2)/P(H_2O)| \geq 1.5 \pm 0.5$$
$$(\text{where } P(H_2) > 2 \text{ Torr}) \quad (5)$$

Equation (5) reflects the fact that a very small concentration of water in hydrogen is sufficient to prevent direct reaction with the metal surface and massive hydriding. However, at the points where the 'breakdown process' occurs and a direct reaction with hydrogen gas is initiated, rapid hydrogen permeation proceeds and surface hydride forms at those heterogeneously distributed locations.

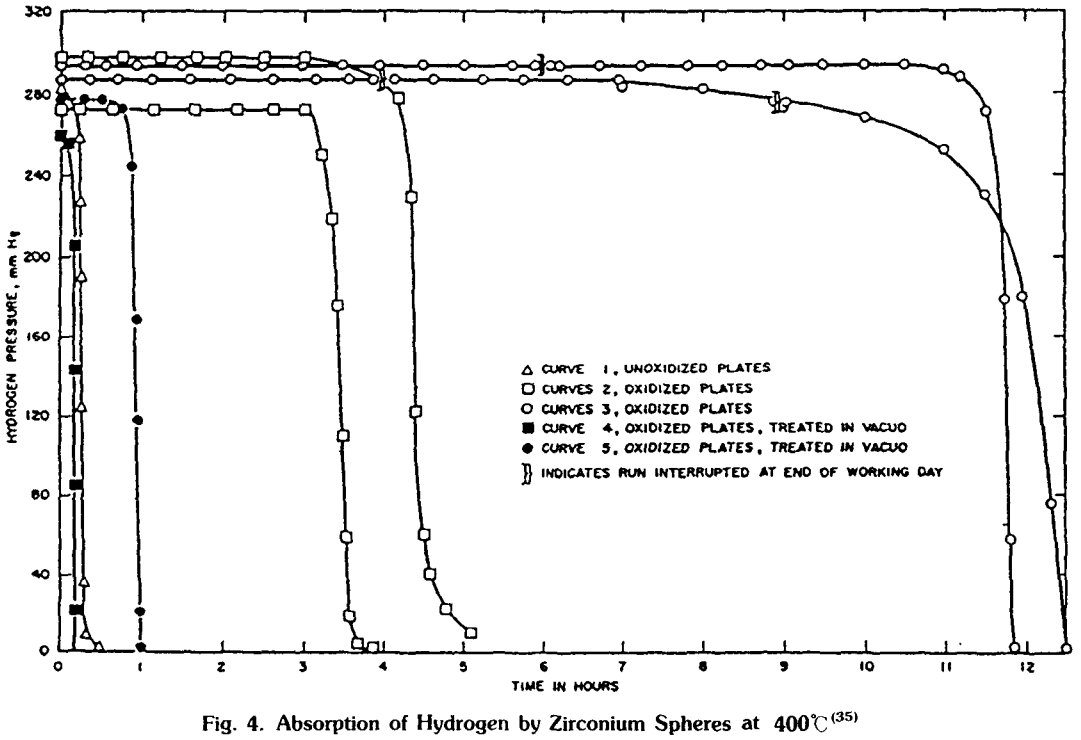

Fig. 4. Absorption of Hydrogen by Zirconium Spheres at 400℃[35]

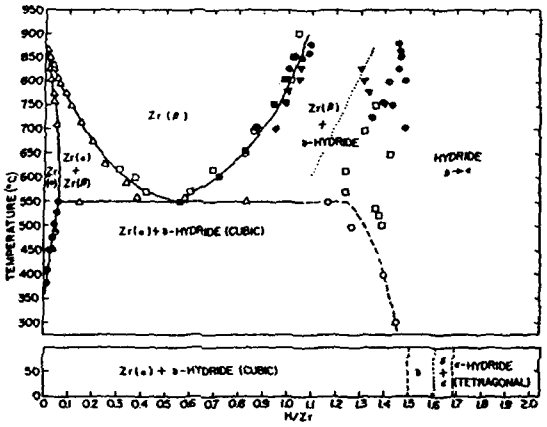

Fig. 5. Zirconium-Hydrogen Phase Diagram[47]

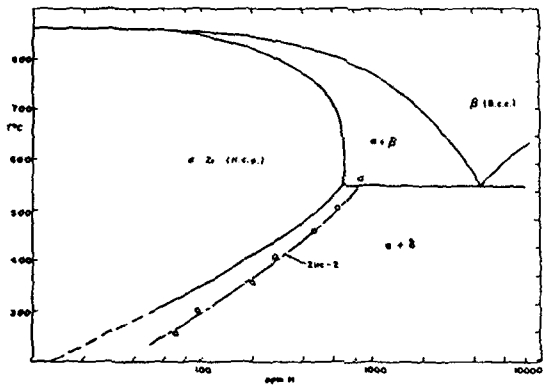

Fig. 6. Zirconium(α Phase)-Hydrogen Phase Diagram[23]

Clayton[8] has provided a more extensive comparison of zircaloy hydriding than the database available to Zima[24].

Terminal Solubility of Hydrogen

The zircaloy hydriding reaction is reversible and strongly dependent on temperature and pressure :

$$Zr+H_2 \leftrightarrow ZrH_2 \quad (6)$$

A considerable amount of work[47-54] has been done on this Zr-H system although there is still no universal agreement on the exact location of the various phase fields in the system. Figure 5 gives a complete composite phase diagram suggested by Libowitz[47], although the location of the $(\beta+\delta)/\delta$ boundary is not well-defined. The exact composition-temperature relationships of the $(\delta+\varepsilon)$ region are still unknown.

The terminal solubility of hydrogen in α-zirconium has been extensively studied[49-54]. The Zr (α)-H equilibrium diagram is shown in Figure 6. Figures 5 and 6 show that at room temperature the terminal solubility of hydrogen is a few ppm and at the operating temperature of 300℃ the solubility limit is around 200 ppm. The experimental points in the diagram are Sawatzky's data for hydrogen in reactor-grade Zircaloy-2[50].

A least-square analysis of all experiment data for α-Zr gives the following relation : solubility (ppm) $=1.61\times10^5$ exp(−8950/RT). There seems to be good agreement among the various investigators. The reported solubilities in the zircaloys, however, represent a difference of a factor of two, the results of Sawatzky[50] and Östberg[51] being the highest. Stating that the technique used by Östberg and Sawatzky led to the supersaturation effect and hence to the high solubilities, Kearns determined the solubility of zircaloys without Östberg's and Sawatzky's data, which turned out to be very close to that for pure zirconium[52].

Grain size and cold work had virtually no effect on either solubility or partitioning among the components of a diffusion couple.

3. Effects of Hydriding on the Mechanical Properties of Zircaloy Cladding

It is well-established that embrittlement of zirconium by hydrides is caused by the presence of the brittle hydride phase, low critical stress intensity factor due to localized hydrogen at the crack tip, or gross embrittlement due to high hydrogen concentration[55-58]. Important factors are the hydride morphology (size and orientation) and the

metal crystallographic characteristics (texture and grain size)[59-61].

Hydride Precipitatio

Above a critical pressure in equation (6), saturation of hydrogen absorption on the zircaloy surface occurs very rapidly and is followed by uniform hydride formation[28,50]. The hydrogen present in quantities above the solubility limit is precipitated as zirconium hydride. Various types of zirconium hydrides are formed, as shown in the Zr-H phase diagram (Figure 5). In zircaloy cladding under operational conditions, δ hydride precipitates are normally observed[47].

The form and morphology of hydrogen precipitates are influenced by metallurgical factors such as texture, grain size, and nature of stresses in the tubing[16,62-65]. Ells[16] thoroughly reviewed and discussed hydrogen precipitation in zirconium alloys. He claimed that needle-like single-phase hydrides were observed in all experiments even with hydrogen concentrations as low as a few tens of ppm. With increasing hydrogen concentration and decreasing cooling rates the hydride needles become platelets. If the cooling rate is sufficiently slow, then the grain boundaries are the preferred sites of nucleation. It seems likely that the primary habit plane is $\{10\bar{1}0\}$ in pure zirconium and $\{10\bar{1}7\}$ in Zircaloy-2 and Zircaloy-4.

Examination of hydrided specimens of polycrystalline zircaloy often reveals that the hydride platelets are oriented parallel to a particular direction. Under reactor operating conditions hydrogen in zircaloy cladding precipitates in the form of platelets in three types of orientation : radial, circumferential and random. The mechanical properties of zircaloy are affected significantly by the presence and orientation of hydride precipitates. The first deleterious effect of oriented hydrogen precipitates was reported in 1961[66]. Radially-oriented hydrides have the most significant effect on tube ductility because they act as crack initiation sites[67]. Thus current industry specifications require that not more than 30% of the platelets shall be oriented less than 40° from the radial direction[68].

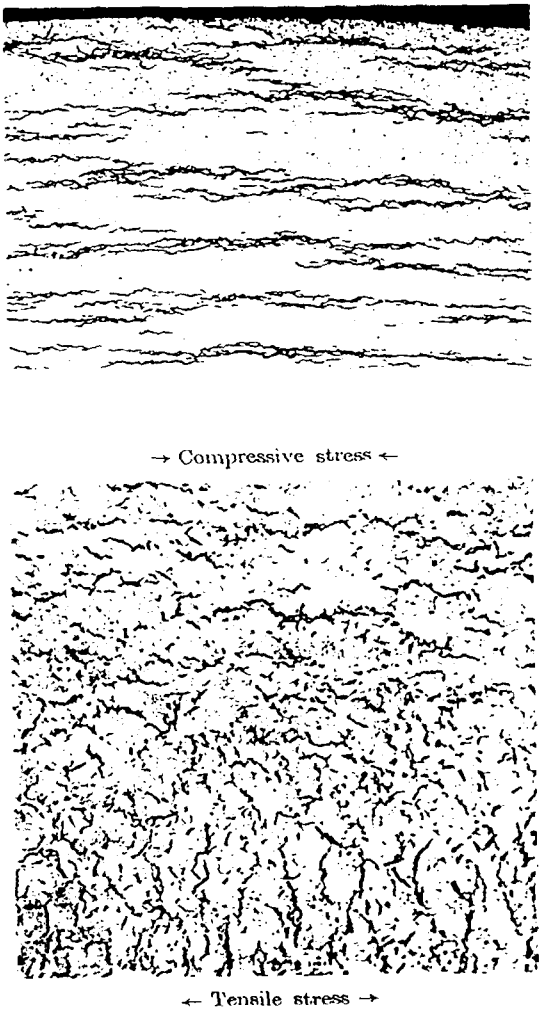

Fig. 7. Hydride Orientation about 200 ppm (a) Circumferential Hydride Under No Strss (× 200)[68] (b) Stress Reorientation of Hydride (× 100)[17]

It is well-known that under certain conditions hydride orientation in zircaloy is dependent on the external stress applied to the specimen during cooling. In regions of compressive stress the hydrides are parallel to the stress axis, while in regions of tensile stress they are perpendicular to

the stress axis. Figure 7a shows the circumferential hydrides of a typical tubing with no applied stress, whereas Figure 7b shows re-orientation of hydrides according to applied stress. The stress condition of internally-pressurized tubes tends to orient hydrides in radial planes, precisely where they pose the most serious threat to tube ductility.

Effect of Hydrides on the Ductile-Brittle Transition Temperature

In the early 1950s it was found that certain zirconium ingots exhibited lower notch-impact energy values than expected, which appeared to be related to an appreciable hydrogen content[56]. Zirconium has excellent resistance to impact, even below room temperature, when little or no hydrogen is present in the metal. When the hydride volume fraction is greater than a critical value, the ductility of the hydride controls the behavior of zirconium and its alloys. The critical value is often related to the formation of a continuous network of hydrides which brittle fracture follows.

Recently Bai et al.[69] published experimental results on the ductile-brittle transition in Zircaloy-4 in the presence of hydrides. At room temperature, the effect of increasing hydrogen concentration on strength (yield and tensile) is not significant. Ductility, on the other hand, is drastically reduced when a critical hydrogen concentration is reached. The critical value varies depending on thermo-mechanical treatment, being about 600 ppm for stress-relieved Zr sheet (0.5 mm thickness), 700 ppm for recrystallized sheet, and less than 250 ppm for β-treated sheet. However, at 350℃ all the specimens remain ductile up to 1000 ppm, which is higher than the concentration that causes the ductile-brittle transition at 20℃. Bai also claimed that when the hydrogen concentration reaches about 2000 ppm the ductility of the Zircaloy-4 is reduced to zero even at 350℃[70]. Fractographic analysis confirmed that the fracture is of the ductile type with cavity nucleation and coalescence with low and medium hydrogen concentrations while the fracture path follows the continuous interfacial-hydride network for specimens with very high hydrogen concentrations.

The oriented hydrides have a noticeable influence on the yield and tensile strength of Zircaloy-4 sheets. For specimens containing 110 ppm H, the elongation is reduced from 30% to 15% at room temperature if the hydrides are oriented[69]. The axial fracture toughness of Zircaloy-2 tube has also been shown to be significantly reduced by the presence of coarse radial-axial precipitates of zirconium hydride[71]. Zirconium hydrides induce cleavage cracks ahead of the crack tip, resulting in a sharp ductile-brittle fracture transition for hydrogen concentrations $\geq$ 60 ppm.

Hydrogen-Assisted Cracking (Hydride Cracking)

Hydride growth kinetics in crack initiation suggests that hydrogen buildup at an arrested crack-tip by diffusion is followed by hydride cracking[57]. At a given stress level and temperature at a crack-tip, the incubation time for cracking depends on the amount of hydrogen available for the formation of hydrides. The stress at the tip of the growing hydride causes hydrogen flow from the surrounding zirconium matrix (stress-directed diffusion of hydrogen). As the local concentration in the matrix drops below the terminal solubility, the hydrides in the bulk dissolve and contribute to the hydrogen flow towards the crack-tip. Hydrogen precipitates at the tip and forms a hydride whose orientation is in the same direction as that of crack propagation. Crack initiation occurs at a critical hydride length.

4. Descriptive Mechanism of Internal Hydriding

Fuel Rod Failure Due To Internal Hydriding

Hydrogen generated inside a fuel rod will ultimately hydride the zircaloy cladding regardless of

its initial chemical state. As long as the hydrogen pick-up is uniform, no significant consequences arise. However, if the hydrogen pick-up is locally enhanced, high concentrations of hydride tend to form at these points. Clayton[8] has categorized hydrogen pick-up by zircaloy clad rods into three groups based on the extent of hydrogenation :

- 'expected' hydriding (50~500 ppm) due to the pick-up fraction of free hydrogen produced in the Zr-H_2O reaction,
- 'accelerated' hydriding (several 1000 ppm) which is hydrogen absorption far in excess of that expected from corrosion, and
- 'massive' hydriding (δ-phase, 16,300 ppm) due to grossly accelerated hydrogen pick-up.

Massive localized hydriding leads to hydride blisters with the volume changes visually evident on the outside of the fuel rod. Ultimate deterioration of the mechanical properties of the cladding is splits or small cracks that eventually perforate the cladding locally.

The failure process due to internal hydriding proceeds through three stages which are shown in Figure 8[3,72,73]. In the initial stage (Figure 8a), localized hydriding on the inner surface of the cladding occurs by mechanisms that will be discussed in the following section. In the second stage (Figure 8b), the hydrided region of radial orientation with radial cracking grows along the inner side. Migration of hydrogen towards the outer surface of the cladding by thermal diffusion leads to formation of massive hydrides. The radially-oriented hydride platelets are called 'sunbursts'. Increased migration of hydrogen to the cooler outer side brings about hydride blistering at both side of the cladding. In the last stage (Figure 8c), transfer of the hydride sunburst to the outer side is completed and a through-wall crack is propagated under the local stress field. This eventually leads to a perforation of the cladding as mentioned in the previous section.

The initiation of massive hydride defects can occur at any stage in fuel operation, but generally occur early in life[3]. This type of damage generally, but not always, will proceed to cladding failure. Hydrided cladding may operate for years without failure if there is no power cycling during operation[72].

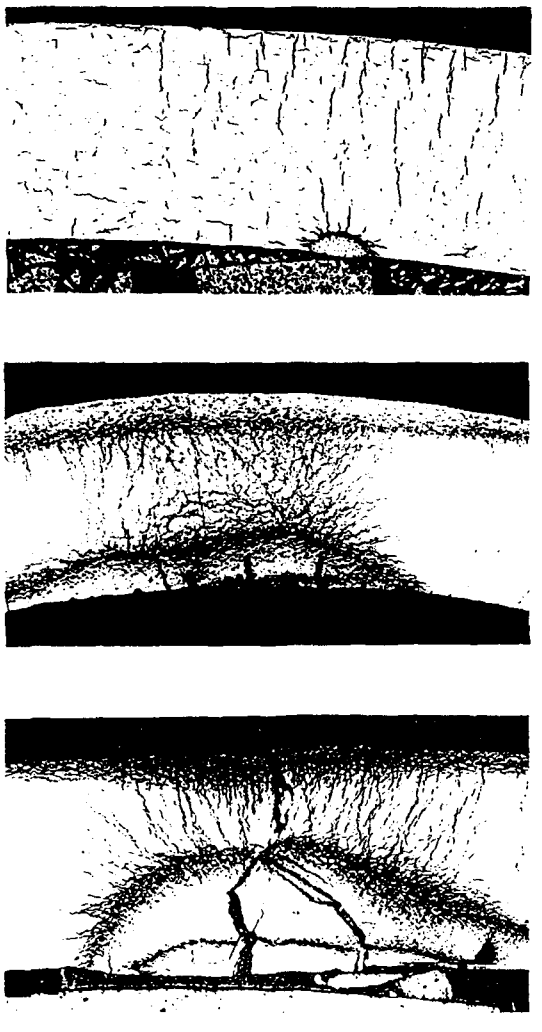

Fig. 8. (a) Early Stage of 'Sunburst' Formation[73]
(b) 'Sunburst' Through the Cladding Wall[3]
(c) Brittle Cracks Propagating Through Hydride 'Sunburst' Reging[73]

Secondary Hydriding in Defected Zircaloy Fuel Rods

Occasionally, the small primary defect leads to heavy secondary hydride formation. Markowitz[21] proposed the first model of the phenomenon which has since been refined by several workers[3,73-75]. Most current theories of hydriding in defected zircaloy rods depend upon one common condition : the corrosive environment (the gas in the fuel-cladding gap) contains insufficient oxidizing power to maintain normal oxidation kinetics ; since the balance of the gas is H_2, accelerated or massive hydriding of the less-protected zircaloy occurs. The descriptive massive hydriding mechanism is as follows :

1. During the initiation stage, water enters the fuel rod and flashes to steam. Pressure equalization occurs between the coolant and the free volume of fuel rod (including the plenum) at the end of this stage. The time for pressure equalization may range from a few minutes to few hours[76] or days[7,75].
2. After the internal and external pressures have equalized, the gaseous products from the fuel rod escape to the coolant. This provides the first evidence of a leaking rod. Erosion and cladding oxidation stress the defect area and mechanically enlarge the primary defect.
3. Steam oxidizes the internal zircaloy cladding surface to ZrO_2, resulting in the release of hydrogen. Some steam is radiolytically decomposed to hydrogen and hydrogen peroxide.
4. Hydrogen from the cladding corrosion reaction is augmented by hydrogen produced by coolant radiolysis and by fuel oxidation. Hydrogen from corrosion, radiolysis, and fuel oxidation described in Section II combine to reduce the steam partial pressure.
5. Hydrogen absorption by the cladding in the gap allows more coolant to flow inward to equalize the pressure. The rate of coolant flow inward is adjusted to match the hydrogen consumption rate by hydriding.
6. As the gases (initially mainly steam) react in the fuel-cladding gap, the concentration of hydrogen continually increases. At peak power and heat flux positions, the oxide layer formed is hottest and its self-healing properties are greatest. However, the cladding thermal gradient is highest at the peak heat flux positions and thus thermal diffusion of any absorbed hydrogen to the outer cladding surface is greatest.
7. As the gas transports beyond peak power and heat flux positions, it becomes more enriched in hydrogen. Oxidation of the internal cladding surface becomes slower and any defects in the oxide film are less likely to heal. At some point along the gas diffusion path H_2O/H_2 ratio reaches the 'critical ratio' which can cause high hydrogen pick-up.
8. Conditions for accelerated hydriding and massive hydriding in localized areas may be achieved at some point along the internal zircaloy cladding surface. Such hydriding could occur at a defect or discontinuity in the ZrO_2 layer or at a region where the protective oxide is thin. At that point the internal hydriding failure mechanism described in the previous section becomes significant. The secondary defect is remote from the primary defect and probably at a region past the peak power or maximum heat flux positions.

5. Discussion

When water enters a perforated fuel rod, the corrosion rate with steam at the inside of the cladding is larger than at the outside of the cladding because of its higher temperature (350~430℃) at the former location. According to Garzarolli, *et al.*[3], a uniform oxide layer is mainly formed and its thickness decreases rapidly with distance from the defect. From this it can be infer-

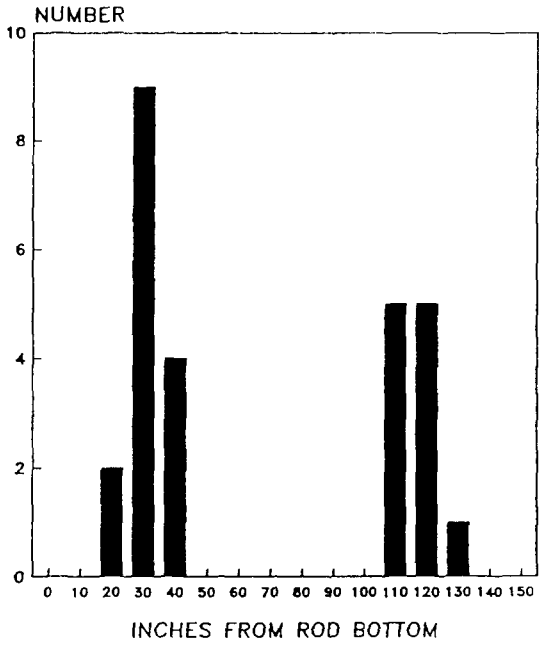

Fig. 9. Axial Location of Through-Wall Defects Due To Secondary Hydriding[6]

red that the supply of oxidant is limited to the area near the perforation as a consequence of gap closure and steam starvation. Besides the uniform oxide layer, local oxide patches with thickness up to 300 /*m are occasionally observed opposite radial pellet cracks. It is suggested that these oxide patches are the result of local depassivation of the uniform oxide layer by reactive fission products like iodine and cesium. This observation suggests a supplementary mechanism of secondary hydriding enhancing the basic steam starvation mechanism.

Regardless of the location of the primary defect, the through-wall defects due to secondary hydriding fall into two distinct groups with respect to axial location on the rods. Figure 9 shows a typical statistics of axial locations of secondary defects[6]. This strongly suggests that gas mixture transport processes in the gap play a significant role in establishing steam starvation.

The increase in O : U ratio in the defective fuel rod is most pronounced at the outer surface of the pellets[3]. A dense surface layer (probably U_3O_8) is often found in ceramographic cross sections of pellets from defective rods. The thickness of this layer varies, depending on the type of defect and the rod power. The U_3O_8 layer is thin (10–30 /*m) with small cladding defects, even after one year of operation. Thick U_3O_8 layers (up to 1000 /*m) develop at large cladding defects. However, in low-rated fuel rods they rapidly decrease in thickness with distance from the defect. Only in high-rated fuel rods the U_3O_8 layer extends over longer distances from the position of the cladding perforation. The increase in stoichiometry results in a decrease in thermal conductivity of the UO_2[77] and, consequently, in a rise of the pellet center temperature. Another consequence of the increase in the O : U ratio and of the formation of an U_3O_8 layer is a diameter increase (maximum 100 /*m) of a defected fuel rod[3].

Factors Affecting Internal Hydriding in Defective Zircaloy Fuel Rods

Defect Size

Intentionally-defected test rods usually exhibited expected hydriding or accelerated hydriding rather than massive hydriding, since sufficient oxidant is present at all times during operation because of the relatively large defect size. Also small pinholes or cracks in operationally-defected fuel rods do not always lead to excessive hydriding. It has been shown that defects can reseal themselves with corrosion products shortly after cladding breach with little or no hydride damage[74,75,78]. Some cladding cracks may be sufficiently tight to prevent coolant penetration[79]. However, it is more likely that operational in-pile defects will enlarge by crack extension or erosion[3,73-75].

A relationship between defect size and hydrogen pick-up was noted in out-of-pile burst tests on Zircaloy-4 rods containing alumina (Al_2O_3) pellets[80]. Higher cladding hydrogen contents

were associated with smaller size rupture openings, which supplied less steam to the inner rod surface. This observation is consistent with the qualitative models discussed above.

Source of Hydrogen

As mentioned in Section II there are four main potential sources of hydrogen inside a defected fuel rod : zircaloy-steam corrosion, dissolved hydrogen in coolant water, radiolysis of steam, and fuel oxidation.

Hydrogen produced by the zircaloy-steam corrosion reaction is picked up again by the underlying zircaloy. The pick-up fraction is usually between 10% and 50% for Zircaloy-2[26] and 5% and 25% for Zircaloy-4[81] depending somewhat on the oxygen content of the water or steam. Also hydrogen can be produced directly by radiolysis and through fuel oxidation by hydrogen peroxide from radiolysis. Radiolytic decomposition of steam in the fuel-cladding gap occurs mostly by fission product recoil. The production of hydrogen by fission-product radiolysis is not an equilibrium process. Hydrogen peroxide molecules can oxidize the fuel even in presence of considerable hydrogen, whereas the presence of hydrogen inhibits the steam oxidation of fuel[7]. Thus the partial pressure ratio, $P(H_2)/P(H_2O)$, is an important parameter. Even ratios as low as $10^{-3}\sim10^{-5}$ are sufficient to inhibit the oxidation reaction. Hydrogen dissolved in the coolant is another possible source especially in pressurized water reactors containing some dissolved hydrogen (Table 1).

Of all the above sources of hydrogen for secondary hydriding, Markowitz claimed that the radiolytic process driving fuel oxidation is the only source that can provide sufficient hydrogen to permit the excessive hydrogenation[21].

Zircaloy Surface Effects

The susceptibility of bare Zr to hydrogen is influenced by the surface treatment of the metal. Mechanically-worked surfaces, such as those abraded, mechanically-polished, and vapor-blasted, sensitize the metal to hydrogen pick-up. Abraded plate specimens exhibited virtually no incubation time in an atmosphere of high purity H_2 at 400℃ and hydriding proceeded uniformly over the entire specimen area. On the other hand, an electro-polished specimen under the same environment exhibited substantial incubation period and hydriding was confined to the edges and corners of specimen[82].

With increasing oxide thickness the incubation time before the onset of the hydriding reaction lengthens[41]. Hydrogen absorption is affected by the type and morphology of the oxide[80]. Generally two mechanisms are advanced to explain how zirconium oxide films permit hydrogen penetration. In one mechanism, mechanical defects such as microcracks, pores, intermetallic particle sites, as well as subgrain boundaries and dislocation networks provide hydrogen with shortcut paths to the zirconium substrate[35,40]. In the other mechanism, presence of substoichiometry in the oxide permits more rapid movement of hydrogen through the oxygen vacancies[26,35,40]. According to this mechanism, very thin films or films under reducing conditions are substoichiometric and thus hydrogen permeates easily, whereas normal-thickness films or films under oxidizing conditions are less permeable[26]. Actually both mechanisms probably operate simultaneously in triggering the internal hydriding reaction.

When nickel-bearing alloys such as Inconel are smeared and bonded onto the surface of a zircaloy component with disrupted or damaged oxide film it acts as a window allowing the ingress of hydrogen to the zircaloy[32].

Heat Flux

It is understood that the higher the heat flux the higher the temperature of the inner cladding surface. Consequently the corrosion film will form

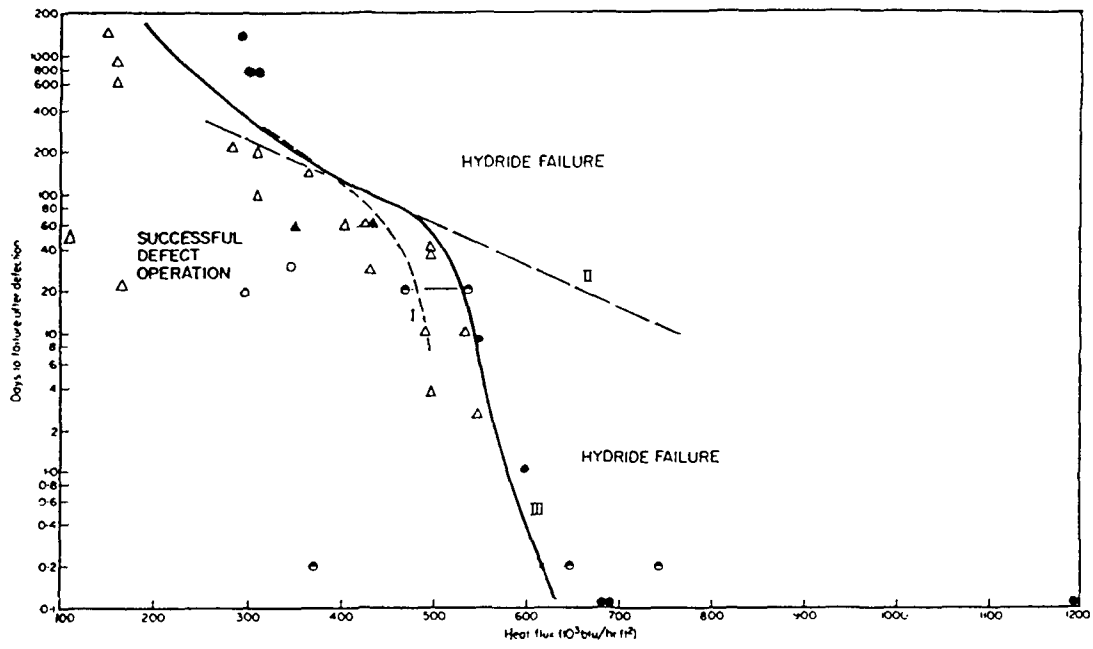

Fig. 10. Assessment of the Failure of Defective Zircaloy Clad Fuel[73]

more rapidly and tend to be more conductive to hydriding, depleting the steam environment and approaching steam starvation conditions earlier.

Locke[73] first attempted to derive a relationship between heat flux and in-pile time for fuel failure, which is shown Figure 10. The clear failure boundary in the figure demonstrates that at high heat flux, the chance of fuel failure due to accelerated and massive hydriding increases and thus the permissible operating time decreases. Locke raised questions based on the operational limit curve in the figure : why is there an apparent critical heat flux range above which defects deteriorate rapidly and how can the two different slopes of the curve be explained? As the cladding temperature is proportional to the heat flux, the two different slopes indicate two distinct activation energies in the zircaloy hydriding, according to temperature range. The steep slope past the critical flux demonstrates a much greater activation energy than that below the critical flux. This suggests more than one mechanism in the reaction.

Hydriding Trends Under Irradiation

One of the operating conditions affecting secondary hydriding is the fast neutron fluence. This parameter is, in fact, correlated with heat flux, which is another operational effect on zircaloy hydriding since heat flux is a direct function of the fission rate in the fuel. Enhanced zircaloy corrosion and hydrogen pick-up was observed as fast neutron fluence increased[31,32,86-90]. Zircaloy-2 hydriding rates were proportional to fast neutron fluence in the oxygenated coolant[89]. This was partially attributed to fast neutron damage of the protective oxide layer[90]. The reduction of fast fluence effect on corrosion enhancement and accelerated hydriding with increasing temperature is explained by damage recovery due to annealing

Aggressive fission products such as iodine and highly energetic and relatively massive fission frag-

ments could damage the resistance of oxide film to hydrogen penetration[3,73,74,83-85].

Redistribution Under the Thermal Gradient and Thermal Cycling

In part, the distribution of corrosion-product hydrogen and its precipitation as hydrides in the cladding are determined by the thermal transport along the temperature gradient across the cladding wall[91-94]. Markowitz[91] demonstrated that under the influence of a temperature gradient, hydrogen in Zircaloy-2 tends to move to the colder regions until a steady state distribution, determined by the so-called heat of transport, is attained. Since then several workers have discussed the thermal diffusion quantitatively and qualitatively[92-94].

Most hydrogen terminal solubility measurements were made without thermal cycling involved. When the specimen was thermally cycled, i.e., thirty times between 50℃ and 400 ℃, the solubility was increased by over 50%. Slow cycling resulted in more supercharging than fast cycling[95]. Westerman[95] explained the phenomena on the basis of thermodynamics and kinetics. Upon slow heating dissolution occurs at the sites of highest hydrogen activity, whereas upon cooling precipitation occurs at thermo-dynamically preferred sites. In this case repeated precipitation will deform the lattice permanently and minimize the strain free energy and thus total free energy may become negative during cycling.

6. Conclusions and Recommendations

Although qualitative understanding of the secondary hydriding mechanism has been achieved over the past three decades it is not enough to support the efforts to mitigate the rash of recent cases of severe degradation of defected fuel rods. In the qualitative model it is assumed that the gas mixture composition is continuously changing along the gap. The $P(H_2)/P(H_2O)$ ratio increases in the gas further from the hole. A drastic change in the $P(H_2)/P(H_2O)$ ratio is assumed to occur in the gas beyond the peak power position, and a critical $P(H_2)/P(H_2O)$ ratio may be achieved. Then massive hydriding occurs. The pressure equilibrium period from the time when the water first enters the rod to the time of pressure equalization is short. It could last only for a few minutes or hours for defect size of about 5×10^{-3} mm diameter and more, up to a few days for smaller pinholes[7]. In any case, the transient period is very short compared to a few months needed for a secondary defect to initiate and to evolve. Therefore it is reasonable to consider other processes that take place during the steady state period. Recently Olander[7] proposed a quantitative model based on gas transport and chemical kinetics.

Precipitation of hydride on the hot inner surface occurs when and where the hydrogen thermal diffusion flux exceeds the 'critical flux' which is a function of the thermal gradient and inner cladding temperature. At any time during operation, the inner and outer cladding surface temperatures can change if the temperature profile along the rod changes as a result of power changes. In this case the hydrogen flux can become higher than the critical flux at a certain axial location in the cladding and hydrogen precipitation would be initiated on the hot inner surface and provide a sink for further hydrogen uptake.

However, it is still not possible to implement a complete quantitative model because of the lack of basic data. A quantitative model requires the following information on the chemistry and gas mixture transport in the gap between cladding and fuel pellet:

- reaction rate laws between $H_2/H_2O/H_2O_2$ gas mixtures and

i) cladding inner wall (temperature of interest: 300~500℃), including dependence on scale thickness

ii) UO_2 fuel at temperatures ranging from 600–1000℃, including the effect of the O : U ratio

• critical H_2, H_2O, and H_2O_2 partial pressures needed for massive hydriding of cladding including effect of hydrogen transport in cladding, and

• radiolysis of gas phase H_2O and stability of H_2O_2 in the gas mixture at high pressures. There is available information for the pure components H_2O and H_2O_2 in the liquid phase but not much for the gas phase and the effect of hydrogen in the gas mixture is not known. Also some information about gas-phase homogeneous thermal decomposition of hydrogen peroxide is available, but not enough for the case of gas mixtures of H_2O, H_2O_2, and H_2 at high pressures.

The following programs to provide with the necessary information are recommended :

a. Investigation of the kinetics of zirconium oxidation and hydriding reactions in mixtures of hydrogen, steam and hydrogen peroxide,

b. Investigation of the oxidation of UO_2 in mixtures of steam, hydrogen and hydrogen peroxide, including oxidation kinetics measurements and the effect of gas composition on oxidation and reduction,

c. Determination of critical $P(H_2)/P(H_2O)$ ratio for accelerated and massive hydriding,

d. Modeling the process of hydrogen penetration, permeation and distribution in the cladding and the process of accelerated and massive hydriding, and

e. Demonstration of the role of radiolytically-produced H_2O_2 by in-reactor testing.

References

1. S.M. Stroller Corp., *EPRI NP-5544* (1987)
2. D.H. Locke, *Nucl. Eng. Desg.*, **33**, 94 (1975)
3. F. Garzarolli, R. von Jan, and H. Stehle, *Atomic Energy Review*, **17**, 31 (1979)
4. A. Jonsson, L. Hallstadius, B. Grapen-giesser, and G. Lysell, *Fuel for the 90's : ANS/ENS International Topical Meeting on LWR Fuel Performance, Avignon, France*, **Vol. 1**, 371 (April 1991)
5. J.H. Davies and G. A. Potts, *Fuel for the 90's : ANS/ENS International Topical Meeting on LWR Fuel Performance, Avignon, France*, **Vol. 1**, 272 (April 1991)
6. Babcock & Wilcox, *EPRI NP-6285-M* (1989)
7. S. Vaknin and D. R. Olander, *EPRI RP-1250-23* (1992)
8. J.C. Clayton, *Zirconium in the Nuclear Industry : Eighth International Symposium, ASTM STP 1023*, 266 (1989)
9. B. Lustman, M. L. Bleiberg, E. S. Byron, J. N. Chirigos, J. G. Goodwin, and G. J. Salvaggio, *Nucleonics*, **19**, 58 (1961)
10. W. R. Thomas, *Fuel Element Fabrication with Special Emphasis on Cladding Materials : Proceedings of a Symposium Held in Vienna, May 10-13, 1960 for IAEA*, **Vol. 1**, 3 (1961)
11. J.N. Chirigos, S. Kass, W. W. Kirk, and G. J. Salvaggio, *Fuel Element Fabrication with Special Emphasis on Cladding Materials : Proceedings of a Symposium Held in Vienna, May 10-13, 1960 for IAEA*, **Vol. 1**, 19 (1961)
12. R.G. Fleck, E.G. Price, and B.A. Cheadle, *Zirconium in the Nuclear Industry : Sixth International Symposium, ASTM STP 824*, 88 (1984)
13. G.P. Sabol, G.R. Kilp, M.G. Balfour, and E. Roberts, *Zirconium in the Nuclear Industry : Eighth International Symposium, ASTM STP 1023*, 227 (1989)
14. S. Kass, *Corrosion of Zirconium Alloys, ASTM STP 368*, 3 (1963)
15. Th. Andersson and G. Vesterlund, *Zirconium in the Nuclear Industry : Fifth International Symposium, ASTM STP 754*, 75 (1982)
16. J.J. Kearns and C.R. Woods, *J. Nucl. Mater., 20*, 241 (1966)
17. C.E. Ells, *J. Nucl. Mater.*, **28**, 129 (1966)

18. E.D. Hindle and G.F. Slattery, *J. Inst. Metals*, **94**, 245 (1966)
19. D.O. Hobson, *Application-Related Phenomena for Zirconium and Its Alloys, ASTM STP 458*, 37 (1969)
20. J.H. Schemel and R.W. McKenzie, *Zirconium in Nuclear Application, ASTM STP 551*, 169 (1974)
21. J. M. Markowitz, *WAPD-TM-351* (1963)
22. K.M. Goldman and D.E. Thomas, *WAPD-MM-184* (1953)
23. G.J. Biefer, L.M. Howe, A. Sawatzky, and F. H. Krenz, *AECL-919* (1959)
24. G.E. Zima, *HW-66537* (1960)
25. F.H. Krenz, *AECL-1626* (1962)
26. E. Hillner, *WAPD-TM-411* (1964)
27. D.W. Freer, D.R. Silvester, and J. N. Wanklyn, *Corrosion, 21*, 137 (1965)
28. R.P. Marshall, *J. the Less Comm. Metals*, **13**, 45 (1967)
29. E. Hillner, *Zirconium in Nuclear Applications, ASTM STP 551*, 449 (1974)
30. K. Videm, *Nucl. Eng. Desg.*, **33**, 170 (1975)
31. E. Hillner, *Zirconium in the Nuclear Industry : Fifth Conference, ASTM STP 754*, 450 (1982)
32. Battelle Pacific Northwest Lab., *EPRI NP-5132* (1987)
33. E. A. Gulbransen and K. F. Andrew, *J. Electrochem. Soc.*, **101**, 348 (1954)
34. R.F. Boyle and T. J. Kisiel, *WAPD-BT-10*, 31 (1958)
35. S. Aronson, *WAPD-BT-19*, 75 (1960)
36. R.E. Westerman, *HW-73511* (1962)
37. D.W. Shannon, *Corrosion*, **19**, 414 (1963)
38. W. Debray, L. Stieding, and U. Rosler, *Electrochem. Tech.*, **4**, 113 (1966)
39. T. Smith, *J. Nucl. Mater.*, **18**, 323 (1966)
40. J. N. Wanklyn, *Electrochem. Tech.*, **4**, 81 (1966)
41. K. Une, Kinetics of Reaction of Zirconium Alloy with Hydrogen, *J. the Comm. Metals*, **57**, 93 (1978)
42. H. Uetsuka, T. Furuta, and S. Kawasaki, *J. Nucl. Sci. Technol.*, **19**, 158 (1982)
43. B.D. Warr, M.B. Elmoselhi, S.B. Newcomb, N.S. McIntyre, A.M. Brennenstuhl, and P.C. Lichtenberger, *Zirconium in the Nuclear Industry : Ninth International Symposium, ASTM STP 1132*, 740 (1991)
44. J.P. Pemsler, *J. Electrochem. Soc.*, **105**, 315 (1958)
45. J.P. Pemsler, *J. Nucl. Mater.*, **7**, 16 (1962)
46. B. Cox, *AECL-8702* (1985)
47. G.G. Libowitz, *J. Nucl. Mater.*, **5**, 228 (1962)
48. C.E. Ells and A.D. McQuillan, *J. Inst. Metals*, **85**, 89 (1956-57)
49. E.A. Gulbransen and K.F. Andrew, *Trans. AIME*, **203**, 136 (1955)
50. A. Sawatzky, *J. Nucl. Mater.*, **2**, 62 (1960)
51. G. Ötberg, *J. Nucl. Mater.*, **5**, 208 (1962)
52. J.J. Kearns, *J. Nucl. Mater.*, **22**, 292 (1967)
53. A. Sawatzky and B.J.S. Wilkins, *J. Nucl. Mater.*, **22**, 304 (1967)
54. G.F. Slattery, *J. Inst. Metals*, **95**, 43 (1967)
55. C.E. Coleman and D. Hardie, *J. the Less Comm. Metals*, **2**, 168 (1966)
56. W.L. Mudge Jr., *Zirconium and Zirconium Alloys, Amer. Soc. Metal*, 146 (1953) (U.S.A.E.C. Report No. *WAPD-T-20*, (1952))
57. A.F. Shalabi and D.A. Meneley, *J. Nucl. Mater.*, **173**, 313 (1990)
58. D.O. Northwood and U. Kosasih, *Int. Metals Rev.*, **28**, 92 (1983)
59. M.P. Puls, *Metal. Trans. A*, **19A**, 1507 (1988)
60. S. Lin, M. Hamasaki, and Y. Chuang, *Nucl. Sci. Engr.*, **71**, 251 (1979)
61. R.P. Marshall and M.R. Louthan Jr., *Trans. ASM*, **56**, 693 (1963)
62. M.R. Louthan and P.R. Marshall, *J. Nucl. Mater.*, **9**, 170 (1963)
63. C.D. Cann, M.P. Puls, E.E. Sexton, and W.G Hutchings, *J. Nucl. Mater.*, **126**, 197 (1984)
64. C.E. Ells, *J. Nucl. Mater.*, **35**, 306 (1970)
65. M. Leger and A. Donner, *Can. Metal. Quar.*

24, 235 (1985)
66. E.I. du Pont de Nemours & Co., *Pregress Report (March 1961), AEC Research and Development Report, DP-605* (1961)
67. W. Evans and G.W. Parry, *Electrochem. Tech.*, **4**, 225 (1966)
68. Sandvik Special Metals Co., *Zirconium Alloy Fuel Clad Tubing : Engineering Guide, 1st ed.* (1989)
69. J. Bai, C. Prioul, J. Pelchat, and F. Barcelo, *Fuel for the 90's : ANS/ENS International Topical Meeting on LWR Fuel Performance, Avignon, France,* **Vol. 1**, 233 (April 1991)
70. J.B. Bai and D. Francois, *J. Nucl. Mater.*, **187**, 186 (1992)
71. P. H. Davies and C. P. Stearns, *Fracture Mechanics : Seventeenth Volume, ASTM STP* **905**, 379 (1986)
72. D.O. Pickman, *Nucl. Engr. Desg.*, **33**, 141 (1975)
73. D.H. Locke, *Nucl. Engr. Desg.*, **21**, 318 (1972)
74. J.H. Davies, *Trans. ANS*, **41**, 269 (1982)
75. D.H. Locke, *IAEA Specialists Meeting on Behavior of Defected Zirconmium Alloy Clad Ceramic Fuel in Water Cooled Reactors, Chalk River, Ontario, Canada, (Sept, 1979), IWGRPT-6* (1980)
76. W.D. Lees, Memorandom to J. C. Wood, *CRNL-1855* (1977)
77. H. Stehle, H. Assmann, and F. Wunderlich, *Nucl. Engr. Desg.*, **33**, 230 (1975)
78. G.G. Bond, D. Cordall, R.M. Cornell, W.N. Fox, A. Garlick, and D.A. Howl, *J. Brit. Nucl. Ener. Soc.*, **16**, 225 (1977)
79. J.C. Clayton, *WAPD-TM-1604* (1987)
80. T. Furuta, S. Kawasaki, M. Hashimoto, and T. Omoto, *J. Nucl. Sci. Technol.*, **15**, 736 (1978)
81. H. Stehle, W. Kaden, and R. Manzel, *Nucl. Engr. Desg.*, **33**, 155 (1975)
82. E.A. Gulbransen and K.F. Andrew, *J. Electrochem. Soc.*, **104**, 709 (1957)
83. R.A. Proebstle, J.H. Davies, T.C. Rowland, D.R. Rutkin, and J.S. Armijo, *Proceedings of CNA/ANS Joint Topical Meeting on Commercial Nuclear Fuel Technology Today,* Toronto, Canada (April,1975)INIS-mf-3193, **Vol. 2**, 15 (1976)
84. R. Haddad and B. Cox, *J. Nucl. Mater.*, **138**, 81 (1986)
85. B. Cox, B.A. Surette, and J.C. Wood, *J. Nucl. Mater.*, **138**, 89 (1986)
86. J.C. Clayton and R.L. Fischer, *Proceedings of the ANS Topical Meeting on Light Water Reactor Fuel Performance, CONF 850401,* **Vol. 1**, Orlando, FL, 3.1 (1985)
87. T.D. Pyecha, G.M. Bain, W.A. McInteer, and C.H. Pham, *Proceedings of the ANS Topical Meeting on Light Water Reactor Fuel Performance, CONF 850401,* **Vol. 1**, Orlando, FL, 3.17 (1985)
88. F. Garzarolli, R.P. Bodner, H. Stehle, and S. Trapp-Pritsching, *Proceedings of the ANS Topical Meeting on Light Water Reactor Fuel Performance, CONF 850401,* **Vol. 1**, Orlando, FL, 3.55 (1985)
89. A.B. Johnson Jr. and J.E. Irwin, *BNWL-463* (1967)
90. R.C. Asher and T.B.A. Kirstein, *J. Nucl. Mater.*, **49**, 105 (1973)
91. J.M. Markowitz, *WAPD-TM-104* (1958)
92. P.G. Shewmon, *Trans. AIME*, **212**, 642 (1958)
93. A. Sawatzky, *J. Nucl. Mater.*, **2**, 321 (1960)
94. C.F. Bilsby, *J. Nucl. Mater.*, **68**, 1 (1977)
95. B. Westerman, *J. Nucl. Mater.*, **18**, 31 (1966)